

**Supporting Information: Thermal transport at solid-nanofluid
interface: from the increase of thermal resistance towards the
shift of rapid boiling**

Haoxue Han,¹ Samy Merabia,² and Florian Müller-Plathe¹

¹*Eduard-Zintl-Institut für Anorganische und Physikalische Chemie,
Technische Universität Darmstadt. Alarich-Weiss-Straße 8, 64287 Darmstadt, Germany*

²*Institut Lumière Matière UMR 5306 CNRS Université Claude Bernard Lyon 1,
Bâtiment Kastler, 10 rue Ada Byron, 69622 Villeurbanne, France.*

(Dated: May 11, 2017)

I. PARAMETER STUDY OF INTERACTION ENERGIES BETWEEN DIFFERENT COMPONENTS IN THE SOLID-NANOFUID SYSTEM

To reduce the dimension of the parameter space, we determined the values of $\epsilon_{\text{np-liq}}$ that leads to aggregation or separation of the particles in liquid and $\epsilon_{\text{np-sub}}$ that lead to weak or strong binding of the particles to the surface.

When the particle-particle or the particle-substrate distances are less than 1 nm, they are considered to be in contact. The contact probability is defined as,

$$P = \frac{t_c}{t_{\text{tot}}} \tag{1}$$

where t_c is the amount of time when the nanoparticle are in contact with other particles and when they are in contact with the surface, and t_{tot} is the total simulation time.

A. Simulation of contact between nanoparticles.

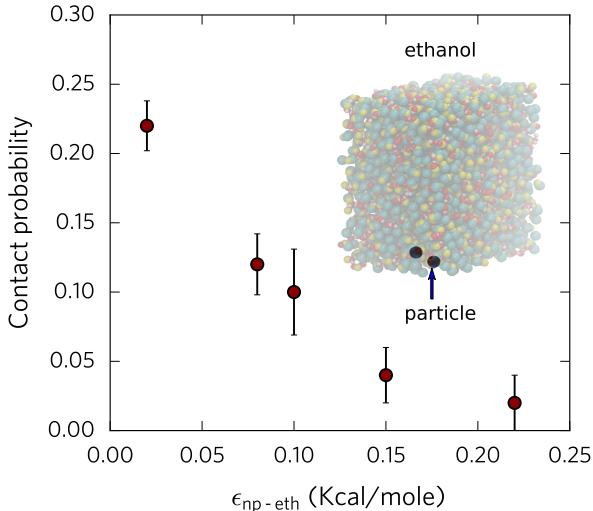


FIG. 1. Probability of contact between nanoparticles versus the particle-ethanol interaction energy $\epsilon_{\text{np-eth}}$.

4600 ethanol molecules (18400 united atoms) are placed in a 3.24 nm-long rectangular periodic cell with a cross-section of 6.48 nm \times 6.48 nm. Two single-site nanoparticles are placed in the liquid. The system is shown in the inset of Fig. 1. A Berendsen thermostat

and Nosé-Hoover-like barostat were used with coupling time constants of 0.2 and 2 ps for temperature and pressure, respectively. A cutoff distance of 1.2 nm for LJ potential and a time step of 0.5 fs were used in all simulations. The Coulomb interaction was truncated with a cutoff distance of 1.4 nm. To equilibrate the system, we first performed molecular dynamics simulations in the constant atom number N , system pressure P and temperature T ensemble (NPT) runs at 1 atm and 300 K for 1 ns. The NPT run was followed by the constant atom number, system volume and temperature (NVT) ensemble run for 1 ns when the temperature was maintained at 300 K using the thermostat. Then, for the following $t_{\text{tot}} = 20$ ns, the thermostats were turned off and the system runs in the constant atom number, system volume and energy (NVE) ensemble. The particle-particle interaction energy was fixed as $\epsilon_{\text{np-np}} = 0.001$ Kcal/mole in the hard-sphere approximation. The distance between the nanoparticles was recorded as a function of time.

The contact probability of the nanoparticles for different particle-liquid interaction energies $\epsilon_{\text{np-eth}}$ was calculated by following its definition in Eq. 1. The result is shown in Fig. 1. When $\epsilon_{\text{np-eth}}$ is small, the nanoparticles tend to be pushed out of the liquid to minimize the total energy of the system. Since the liquid system is periodic, a phase separation between the nanoparticles and the liquid is favored. Hence, the probability of contact between nanoparticles is high, i.e. the nanoparticles tend to aggregate. On the other hand, when $\epsilon_{\text{np-eth}}$ is large, the nanoparticles are well-dissolved in the liquid, resulting in a small contact probability between the particles, as shown in Fig. 1. The distance between the nanoparticles and the substrate was recorded as a function of time.

B. Simulation of contact between nanoparticles and the substrate.

4600 ethanol molecules (18400 united atoms) are placed in a 12.4 nm-long rectangular periodic cell with a cross-section of 3.24 nm \times 3.24 nm in contact with a solid surface. Two single-site nanoparticles are placed in the liquid. The solid has a face-centered cubic (FCC) lattice of 2880 gold atoms, with the (100) surface facing the liquid, and the interaction between gold atoms was also described by a 12-6 LJ potential, as described in the main text of the manuscript. The system is shown in the inset of Fig. 2. The system underwent the same equilibration simulation as in Section I A when the solid and the liquid subsystems are equilibrated with separate thermostats at 300 K. The particle-liquid interaction energy was

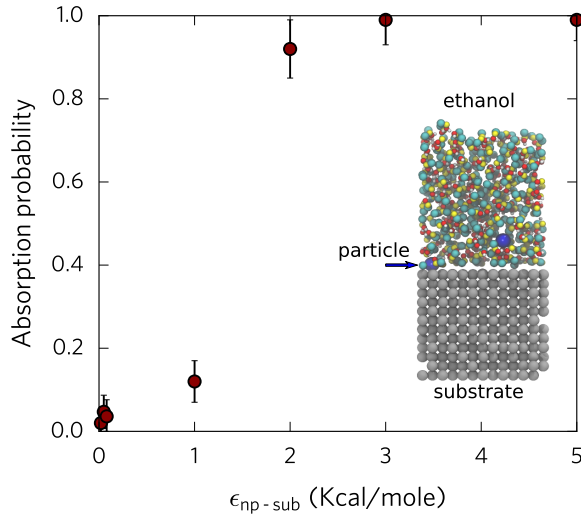


FIG. 2. Probability of contact between nanoparticles and the substrate with versus the particle-substrate interaction energy ϵ_{np-sub} .

fixed as $\epsilon_{np-liq} = 0.2$ Kcal/mole for a good solubility of nanoparticles. The particle-particle interaction energy was fixed as $\epsilon_{np-np} = 0.001$ Kcal/mole in the hard-sphere approximation.

The contact probability of the nanoparticles and the substrate for different particle-substrate interaction energies ϵ_{np-sub} was calculated by following its definition in Eq. 1. The result is shown in Fig. 2. When ϵ_{np-sub} is small, the nanoparticles are well dispersed in the liquid and hence the contact probability is low. On the other hand, when ϵ_{np-sub} is large, the nanoparticles are strongly attracted by the substrate and hence the contact probability is high.

II. PRINCIPLES OF THE THERMAL RESISTANCE AND BOILING SIMULATIONS

We briefly present here the principles of the thermal resistance and the boiling simulations. The system considered for the thermal resistance calculations is schematically represented in Fig. 3. Note that periodic boundary conditions are applied in the directions x and y , but not in the direction z perpendicular to the interface. In this latter direction, a void gap is maintained between the outermost gold atoms and the ethanol suspension. In these simulations, two layers of gold atoms are frozen and ten gold atoms layers are initially

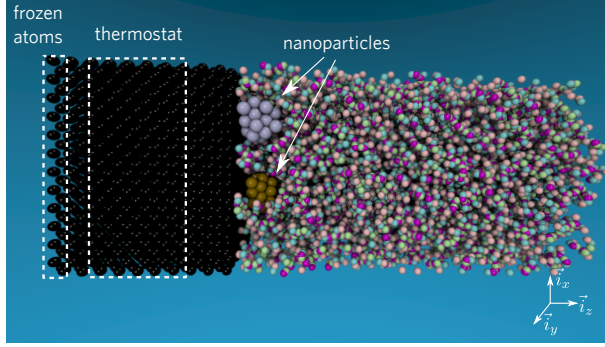


FIG. 3. Cut view of the system considered to compute the thermal resistance between gold and the fluid suspension. Black spheres represent gold atoms, ethanol atoms are represented by coloured small spheres, while nanoparticles are shown as coloured big beads.

thermalized as represented in Fig. 3. After initial heating of the gold atoms, the system is allowed to cool down and the temperature of the gold atoms is monitored as explained in the section IV.

The principle of the boiling simulations is quite similar except that we do not freeze the positions of the outermost gold atoms, and we employ periodic boundary conditions in all directions.

III. LOCAL THERMAL EQUILIBRIUM

In order to confirm local thermal equilibrium, we have calculated the ethanol molecules velocity distribution. The center-of-mass (COM) velocities v (three components along the axes of the Cartesian coordinates) of ethanol molecules inside the bin at the center of the system are recorded and averaged for 500 ps. The histogram of the velocities are shown in Fig. 4. It can be observed that the COM velocity follows the Maxwell-Boltzmann distribution with the probability density of $f(v) = \sqrt{m/2\pi k_B T} \exp(-mv^2/2k_B T)$, where m is the mass of an ethanol molecule, $k_B T$ the Boltzmann constant and T the temperature. The temperature T corresponding to the velocity distribution is determined to be 290 K which agrees relatively well with the local temperature of the central bin.

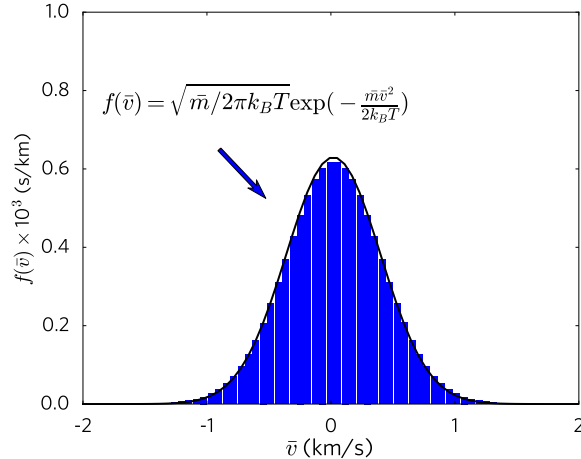


FIG. 4. Velocity distribution of the ethanol molecules calculated in a gold/ethanol suspension interface system with $\epsilon_{\text{np-sub}} = \epsilon_{\text{np-np}} = 0.2$ kcal/mol. The solid line shows the Maxwell-Boltzmann distribution with a temperature $T = 290$ K.

IV. THERMAL RELAXATION METHOD

We used a thermal relaxation method to measure the thermal contact conductance $G = 1/R$ at the solid-liquid interface. The method mimics the thermoreflectance experiment where energy is delivered to the solid over a fraction of a picosecond, which is typically much shorter than the thermal relaxation time. The temperature difference $\Delta T(t)$ between the hot solid and the liquid is shown in Fig. 5. We integrate the normalized temperature difference $\Delta T(t)/\Delta T(0)$ and eventually obtained a plateau, as shown by the green curve. We then plot the exponential decay function,

$$D(t) = T(0) \exp(-t/\tau) \quad (2)$$

where τ is the relaxation time constant extracted from the value of the plateau. Finally, the relaxation time is used in Eq. 1 of the main text to compute the Kapitza conductance.

V. SPECTRAL HEAT FLUX FROM SOLID TO THE LIQUID

The heat flow across the solid-liquid interface is written as,

$$Q = 1/2A \sum_{j \in l} \sum_{i \in s} \langle \mathbf{F}_{ij} \cdot (\mathbf{v}_i + \mathbf{v}_j) \rangle = 1/A \sum_{j \in l} \sum_{i \in s} \langle \mathbf{F}_{ij} \cdot \mathbf{v}_i \rangle$$

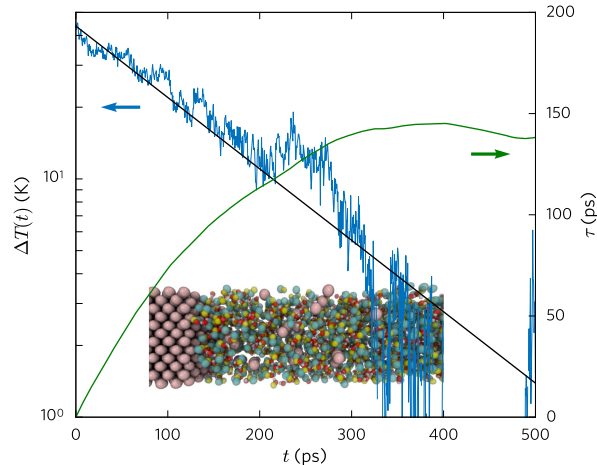


FIG. 5. Relaxation of the temperature difference between the hot solid and the liquid. The blue curve is the temperature difference versus time $\Delta T(t)$. The green curve is the time integral of the normalized temperature difference to extract the decay constant of the temperature difference. The black curve is an exponential decay function of the temperature difference with the time constant extracted from the integral.

where A is the surface area and atomic force \mathbf{F}_{ij} on the solid atom i from the liquid atom j . The heat flux can be decomposed in the spectral space as,

$$Q = \int_0^\infty q(\omega) \frac{d\omega}{2\pi}$$

where $q(\omega)$ is defined in the manuscript.

The spectral heat flux can be calculated in terms of the discrete Fourier transforms of the force and velocity trajectories as¹,

$$q = \frac{2}{AM\Delta t} \Re \sum_{j \in l} \sum_{i \in s} \langle \mathbf{F}_{ij}(\omega) \cdot \mathbf{v}_i^\dagger(\omega) \rangle,$$

where Δt is the sampling interval and M is the sample number. Only the solid atoms located within the potential cutoff of the liquid atoms contribute to the heat flux.

¹ K. Sääskilähti, J. Oksanen, J. Tulkki, and S. Volz, Phys. Rev. E 93, 052141 (2016)